

## Carbon Dioxide/Epoxyde Coupling Reactions Utilizing Lewis Base Adducts of Zinc Halides as Catalysts. Cyclic Carbonate versus Polycarbonate Production

Donald J. Darensbourg,\* Samuel J. Lewis, Jody L. Rodgers, and Jason C. Yarbrough

Department of Chemistry, Texas A&M University, College Station, Texas 77843

Received August 21, 2002

The reactions of zinc halides with 2,6-di-methoxypyridine or 3-trifluoromethylpyridine in dichloromethane have led to the formation of quite different complexes. Specifically, reactions involving pyridine containing electron donating methoxy substituents have provided salts of the type  $[Zn(2,6\text{-dimethoxypyridine})_4][Zn_2X_6]$ , as revealed by elemental analysis and X-ray crystallography. On the other hand, simple bis-pyridine adducts of zinc halides were isolated from the reactions involving the pyridine ligand with electron withdrawing substituents and characterized by X-ray crystallography, for example,  $Zn(3\text{-trifluoromethylpyridine})_2Br_2$ . These zinc complexes were shown to be catalytically active for the coupling of carbon dioxide and epoxides to provide high molecular weight polycarbonates and cyclic carbonates, with the order of reactivity being  $Cl \geq Br > I$ , and 2,6-di-methoxypyridine > 3-trifluoromethylpyridine. Polycarbonate production from carbon dioxide and cyclohexene oxide was shown to be first-order in both metal precursor complex and cyclohexene oxide, as monitored by in situ infrared spectroscopy at 80 °C and 55 bar pressure. For reactions carried out in CO<sub>2</sub> swollen epoxide solutions in the absence of added quantities of pyridine, the copolymer produced contained significant polyether linkages. Alternatively, reactions performed in the presence of excess pyridine or in hydrocarbon solvent, although slower in rate, afforded completely alternating copolymers. For comparative purposes, zinc chloride was a very effective homopolymerization catalyst for polyethers. Additionally, zinc chloride afforded copolymers with 60% carbonate linkages in the presence of high carbon dioxide pressures. In the case of cyclohexene oxide, the copolymer back-biting reaction led exclusively to the production of the trans cyclic carbonate as shown by infrared spectroscopy in  $\nu(C=O)$  region and X-ray crystallography. The unique feature of these catalyst systems is their simplicity.

### Introduction

The utilization of carbon dioxide in the coupling reaction with epoxides to afford polycarbonates and/or cyclic carbonates has received much attention recently. This alternative method of synthesizing polycarbonates to the currently employed industrial process, which involves interfacial polycondensation of phosgene and diols, was first demonstrated by Inoue and co-workers using heterogeneous zinc catalysts in organic solvents.<sup>1</sup> Since this initial discovery, several soluble zinc catalysts have been developed which possess high activity toward the copolymerization of carbon dioxide and *alicyclic* epoxides, for example, cyclohexene

oxide.<sup>2</sup> Specifically, these more recent catalytic processes have been generally performed in subcritical or supercritical carbon dioxide where the catalysts are soluble in the CO<sub>2</sub> expanded epoxide, thus requiring no added organic solvent. In addition, other metal complexes, for example, aluminum-

\* To whom correspondence should be addressed. E-mail: DJDarens@mail.chem.tamu.edu.

(1) Inoue, S.; Koinuma, H.; Tsuruta, T. *J. Polym. Sci., Part B: Polym. Phys.* **1969**, *7*, 287.

(2) (a) Darensbourg, D. J.; Holtcamp, M. W. *Macromolecules* **1995**, *28*, 7577. (b) Super, M.; Berluce, E.; Costello, C.; Beckman, E. *Macromolecules* **1997**, *30*, 368. (c) Super, M.; Beckman, E. *J. Macromol. Symp.* **1998**, *127*, 89. (d) Cheng, M.; Lobkovsky, E. B.; Coates, G. W. *J. Am. Chem. Soc.* **1998**, *120*, 11018. (e) Beckman, E. *Science* **1999**, *283*, 946. (f) Darensbourg, D. J.; Holtcamp, M. W.; Struck, G. E.; Zimmer, M. S.; Niezgodna, S. A.; Rainey, P.; Robertson, J. B.; Draper, J. D.; Reibenspies, J. H. *J. Am. Chem. Soc.* **1999**, *121*, 107. (g) Darensbourg, D. J.; Wildeson, J. R.; Yarbrough, J. C.; Reibenspies, J. H. *J. Am. Chem. Soc.* **2000**, *122*, 12487. (h) Cheng, M.; Moore, D. R.; Reczek, J. J.; Chamberlain, B. M.; Lobkovsky, E. B.; Coates, G. W. *J. Am. Chem. Soc.* **2001**, *123*, 8738. (i) Darensbourg, D. J.; Yarbrough, J. C. *J. Am. Chem. Soc.* **2002**, *124*, 6335. (j) Moore, D. R.; Cheng, M.; Lobkovsky, E. B.; Coates, G. W. *Angew. Chem., Int. Ed.* **2002**, *41*, 2599.

(III) or chromium(III) porphyrinates, have been investigated as catalysts for the coupling of carbon dioxide and epoxides to afford polycarbonates.<sup>3</sup> On the other hand, these and other catalyst systems have been very effective at coupling carbon dioxide and *aliphatic* epoxides, especially propylene oxide, to produce mainly cyclic carbonates.<sup>4</sup>

Nevertheless, synthesis of cyclic carbonates by carbon dioxide/epoxide coupling reactions is of interest because of the use of these compounds in a variety of applications, including high-boiling solvents,<sup>5</sup> additives for hydraulic fluids,<sup>6</sup> and the curing of phenol-formaldehyde resins,<sup>7</sup> plus many more.<sup>8</sup> In this regard, there have been several reports of effective homogeneously catalyzed coupling of epoxides and carbon dioxide to produce cyclic carbonate,<sup>3d,9</sup> including the conversion of chiral oxiranes to chiral cyclic carbonates.<sup>9f</sup> Prominent among these is the recent work of Kim and co-workers.<sup>10</sup> These researchers have described a catalyst system derived from the addition of various pyridine bases to zinc halides salts which effectively catalyzes the coupling of propylene oxide and carbon dioxide to produce cyclic carbonates. Indeed, Kim's study, along with their isolation of a stable pyridinium zinc derivative of the ring opened epoxide, was the inspiration for our investigation of these zinc halides–pyridine adducts for coupling reactions of cyclohexene oxide and carbon dioxide.

## Experimental Section

**Methods and Materials.** Unless otherwise specified, all syntheses and manipulations were carried out on a double manifold Schlenk vacuum line under an argon atmosphere or in an argon filled glovebox. Glassware was flame dried before use. All solvents were freshly distilled prior to being used. Cyclohexene oxide was purchased from Lancaster Synthesis and was distilled from calcium hydride. Anhydrous ZnCl<sub>2</sub> and ZnI<sub>2</sub> were purchased from Aldrich Chemical Co., and anhydrous ZnBr<sub>2</sub> was purchased from Lancaster Synthesis. 3-Trifluoromethylpyridine, 2,6-dimethoxypyridine, 2-phenylpyridine, and 2,6-diphenylpyridine were purchased from Lancaster Synthesis and used as received, as were 2,6-dimethylpyridine

(2,6-lutidine), 2,6-di-*tert*-butylpyridine, and 2,4,6-tri-*tert*-butylpyridine which were purchased from Aldrich Chemical Co. All isotopically labeled solvents for NMR studies were purchased from Cambridge Isotope Laboratories. Infrared spectra and kinetic measurements were monitored on ASI's ReactIR 1000 system equipped with a MCT detector and a 30 bounce SiCOMP in situ probe. <sup>1</sup>H and <sup>13</sup>C NMR spectra were recorded on Unity + 300 MHz or VXR 300 MHz superconducting high resolution spectrometers.

### Reaction of Zinc Bromide with 2,6-Dimethoxypyridine, **1a**.

To a 15 mL CH<sub>2</sub>Cl<sub>2</sub> suspension of ZnBr<sub>2</sub> (0.448 g, 1.99 mmol) was added 2 equiv of 2,6-dimethoxypyridine (0.552 g, 3.97 mmol). The slurry was stirred at room temperature for approximately 12 h after which a fine white powder had precipitated in place of the granular ZnBr<sub>2</sub>. The solvent was removed under vacuum and any unreacted pyridine removed by heating to 40 °C to yield 0.945 g of product (95%). Alternatively, ZnBr<sub>2</sub> was dissolved in diethyl ether, and the product was precipitated upon the addition of the pyridine, followed by washing with ether. This method, however, leads to lower yields presumably due to a sparing solubility of the complex in ether.

Elemental analysis of the white powder was consistent with its formulation as Zn<sub>3</sub>Br<sub>6</sub>(2,6-dimethoxypyridine)<sub>4</sub>. Anal. Calcd for C<sub>28</sub>H<sub>36</sub>O<sub>8</sub>N<sub>4</sub>Br<sub>6</sub>Zn<sub>3</sub>: C, 27.29; H, 2.94; N, 4.55. Found: C, 26.29; H, 2.92; N, 4.37. Colorless, block crystals of **1a** suitable for X-ray analysis were obtained by layering a solution of zinc bromide in diethyl ether with a solution of 2,6-dimethoxypyridine in CH<sub>2</sub>Cl<sub>2</sub> contained in a 1/8 in. sealed glass tube. Alternatively, colorless, block crystals were obtained by slow evaporation of solvent from a concentrated THF solution of the white powder into toluene at –20 °C. X-ray analysis revealed this material to be a THF adduct of Zn<sub>3</sub>Br<sub>6</sub>(2,6-dimethoxy-pyridine)<sub>4</sub>, **1a·2THF**.

The chloride (**1b**) and iodide (**1c**) analogues of complex **1a** were prepared and isolated as white powders in an identical manner to that of **1a** and were shown by elemental analysis to be of similar composition. For example, Anal. Calcd for Zn<sub>3</sub>Cl<sub>6</sub>(2,6-dimethoxypyridine)<sub>4</sub> (**1b**): C, 34.83; H, 3.76; N, 5.80. Found: C, 32.83; H, 3.66; N, 5.47. Furthermore, reactions carried out in a similar manner employing 2,6-substituted pyridines with phenyl, methyl, and <sup>t</sup>Bu groups, as well as 2-phenylpyridine, provided correspondent zinc derivatives.

Employing the published synthetic method for Zn(py)<sub>2</sub>X<sub>2</sub> and Zn(bipy)X<sub>2</sub>, which involves the slow addition of the pyridine ligand to a hot absolute alcohol solution of the zinc halide, provided complexes of the same formulation as **1a**.<sup>11</sup> For example, from the reaction of ZnBr<sub>2</sub> and 2,6-dimethoxypyridine, a white powder was obtained which analyzed to be Zn<sub>3</sub>Br<sub>6</sub>(dimethoxypyridine)<sub>4</sub>. Anal. Calcd for C<sub>28</sub>H<sub>36</sub>O<sub>8</sub>N<sub>4</sub>Br<sub>6</sub>Zn<sub>3</sub>: C, 27.29; H, 2.94; N, 4.55. Found: C, 27.07; H, 3.05; N, 4.40.

**Synthesis of (3-Trifluoromethylpyridine)<sub>2</sub>ZnX<sub>2</sub>, X = Cl (**2a**), Br (**2b**), and I (**2c**).** The preparation of these derivatives was initiated in a manner similar to that utilized for the synthesis of the other pyridine derivatives. For example, to a 15 mL CH<sub>2</sub>Cl<sub>2</sub> suspension of ZnBr<sub>2</sub> (0.217 g, 0.964 mmol) was added 2 equiv of 3-trifluoromethylpyridine (0.283 g, 1.92 mmol). After stirring the reaction mixture for 6 h, the solution became clear and slightly yellow. Upon removal of the solvent under vacuum, 0.386 g (77.2% yield) of (3-trifluoro-methylpyridine)<sub>2</sub>ZnBr<sub>2</sub> was isolated. Anal. Calcd for C<sub>12</sub>H<sub>8</sub>N<sub>2</sub>F<sub>6</sub>ZnBr<sub>2</sub>: C, 27.75; H, 1.55; N, 5.39. Found: C, 27.60; H, 1.62; N, 5.35. Yellow, X-ray quality crystals of the

- (3) (a) Inoue, S. *J. Polym. Sci., Part A: Polym. Chem.* **2000**, *38*, 2861. (b) Mang, S.; Cooper, A. I.; Colclough, M. E.; Chauhan, N.; Holmes, A. B. *Macromolecules* **2000**, *33*, 303. (c) Stamp, L. M.; Mang, S. A.; Holmes, A. B.; Knights, K. A.; de Miguel, Y. R.; McConvey, I. F. *Chem. Commun.* **2001**, 2502. (d) Kruper, W. J.; Dellar, D. V. *J. Org. Chem.* **1995**, *60*, 725.
- (4) Darensbourg, D. J.; Holtcamp, M. W. *Coord. Chem. Rev.* **1996**, *153*, 155.
- (5) Behr, A. *Carbon Dioxide Activation by Metal Complexes*; VCH: Weinheim, 1988; p 7.
- (6) Nankee, R. J.; Avery, J. R. Schrems, J. E. Dow Chem. Patent FR. 15,72,282, 1967; *Chem. Abstr.* **1970**, *72*, 69016p.
- (7) Pizzi, H.; Stephanou, A. *J. Appl. Polym. Sci.* **1993**, *49*, 2157.
- (8) Shaikh, A.-A. G.; Sivaram, S. *Chem. Rev.* **1996**, *96*, 951–976.
- (9) (a) Matsuda, H.; Ninagawa, A.; Nomura, R. *Chem. Lett.* **1979**, 1261. (b) Matsuda, H.; Ninagawa, A.; Nomura, R.; Tsuchida, T. *Chem. Lett.* **1979**, 573. (c) Ratzenhofer, M.; Kisch, H. *Angew. Chem., Int. Ed. Engl.* **1980**, *19*, 317. (d) Nomura, R.; Ninagawa, A.; Matsuda, H. *J. Org. Chem.* **1980**, *45*, 3735. (e) Nomura, R.; Kimura, M.; Teshima, S.; Ninagawa, A.; Matsuda, H. *Bull. Chem. Soc. Jpn.* **1982**, *55*, 3200. (f) Kisch, H.; Millini, R.; Wang, I. *J. Chem. Ber.* **1986**, *119*, 1090. (g) Dümmler, W.; Kisch, H. *Chem. Ber.* **1990**, *123*, 277. (h) Paddock, R. L.; Nguyen, S. T. *J. Am. Chem. Soc.* **2001**, *123*, 11498.
- (10) (a) Kim, H. S.; Kim, J. J.; Lee, B. G.; Jung, O. S.; Jang, H. G.; Kang, S. O. *Angew. Chem., Int. Ed.* **2000**, *39*, 4096. (b) Kim, H. S.; Kim, J. J.; Kwon, H. N.; Chung, M. J.; Lee, B. G.; Jang, H. G. *J. Catal.* **2002**, *205*, 226.

- (11) Postmus, C.; Ferraro, J. R.; Wozniak, W. *Inorg. Chem.* **1967**, *6*, 2030.

Table 1. Crystallographic Data for Complexes **1a**, **1a**·2THF, **2b**, and **8**

	<b>1a</b>	<b>1a</b> ·2THF	<b>2b</b>	<b>8</b>
empirical formula	C <sub>29</sub> H <sub>38</sub> Br <sub>6</sub> Cl <sub>2</sub> N <sub>4</sub> O <sub>8</sub> Zn <sub>3</sub>	C <sub>36</sub> H <sub>52</sub> Br <sub>6</sub> N <sub>4</sub> O <sub>10</sub> Zn <sub>3</sub>	C <sub>12</sub> H <sub>10</sub> Br <sub>2</sub> F <sub>6</sub> N <sub>2</sub> Zn	C <sub>12</sub> H <sub>10</sub> O <sub>3</sub>
fw (g/mol)	1317.10	1376.39	521.41	202.20
T (K)	110(2)	293(2)	293(2)	293(2)
wavelength (Å)	0.71073	0.71073	0.71073	0.71073
cryst syst	triclinic	monoclinic	orthorhombic	orthorhombic
space group	P1	Cc	Fdd2	P2 <sub>1</sub> 2 <sub>1</sub> 2 <sub>1</sub>
a (Å)	14.201(3)	26.607(2)	25.348(4)	6.4041(10)
b (Å)	15.419(3)	14.4148(12)	26.884(4)	9.2575(15)
c (Å)	20.423(4)	15.9052(13)	4.7868(8)	11.7214(19)
α (deg)	86.34(3)			
β (deg)	87.36(3)	125.4240(10)		
γ (deg)	89.29(3)			
cell V (Å <sup>3</sup> )	4457.9(15)	4971.0(7)	3262.1(9)	694.91(19)
Z	4	4	8	4
D <sub>calcd</sub> (mg/m <sup>3</sup> )	1.962	1.839	2.123	1.933
abs coeff (mm <sup>-1</sup> )	7.145	6.311	6.463	0.139
obsd reflns	23,761	15,402	3399	4455
unique reflns (I > 2σ)	15,492	8314	1131	1670
R <sub>w</sub> <sup>a</sup> % [I > 2σ]	9.10	6.94	8.31	3.52
R <sub>w</sub> <sup>a</sup> % [I > 2σ]	19.82	17.97	20.65	10.69

$$^a R = \frac{\sum ||F_o| - |F_c||}{\sum |F_c|} / \frac{\sum |F_o|}{\sum |F_c|}; R_w = \left\{ \frac{\sum w(F_o^2 - F_c^2)^2}{\sum w(F_o^2)^2} \right\}^{1/2}.$$

product were obtained by slow evaporation of a concentrated CH<sub>2</sub>-Cl<sub>2</sub> solution of the complex into toluene at -20 °C.

**Copolymerization of Cyclohexene Oxide/Propylene Oxide and Carbon Dioxide.** A 0.100 g sample of the catalyst complex was dissolved in 20 mL of the appropriate epoxide. The solution was rapidly loaded via an injection port into a 300 mL stainless steel Parr autoclave that had been previously dried overnight at 80 °C under vacuum. The reactor was pressurized to 700 psi with CO<sub>2</sub>, heated to 80 °C, and stirred for 24 h. After that time, the autoclave was cooled and the CO<sub>2</sub> vented into a fume hood. The reactor was opened, and the polymer was isolated from the viscous/solid mixture by dissolution in small amounts of methylene chloride followed by precipitation from methanol.

**Isolation of *trans*-Cyclic Cyclohexylcarbonate, **8**.** This compound was isolated from the reaction mixture of a polymerization process utilizing complex **1a** as a catalyst precursor. Following the removal of high molecular weight polymer by precipitation in methanol, the remaining solution of MeOH and CH<sub>2</sub>Cl<sub>2</sub> was allowed to slowly evaporate in the air to provide crystals suitable for X-ray analysis of the cyclic carbonate.

**Synthesis of *trans*-Cyclic Cyclohexylcarbonate, **8**.**<sup>12</sup> An excess of pyridine (19.5 g, 246 mmol) was added to a 10-mL CH<sub>2</sub>Cl<sub>2</sub> solution of *trans*-1,2-cyclohexanediol (2.49 g, 21.4 mmol) followed by cooling in a dry ice/acetone bath. A 15-mL CH<sub>2</sub>Cl<sub>2</sub> solution of triphosgene (4.17 g, 14.1 mmol) was subsequently added dropwise to give an orange solution, which was allowed to warm slowly to room temperature. The reaction mixture was quenched using saturated aqueous NH<sub>4</sub>Cl followed by extraction of the aqueous phase with CH<sub>2</sub>Cl<sub>2</sub>. The organic extracts were washed with 1 M HCl, saturated NaHCO<sub>3</sub>, saturated NaCl, H<sub>2</sub>O, dried with MgSO<sub>4</sub>, and filtered. Solvent and excess pyridine were removed in vacuo followed by product isolation using a silica gel column and recrystallized in benzene/hexanes to yield 1.52 g (76%). <sup>1</sup>H NMR (CDCl<sub>3</sub>): δ 1.35–2.25 (m, 8H, CH<sub>2</sub>), 3.96 (m, 2H, CH-carbonate). <sup>13</sup>C NMR (CDCl<sub>3</sub>): δ 18.58, 26.12, 75.26, 154.70. IR ν(C=O), CH<sub>2</sub>Cl<sub>2</sub>: 1881 cm<sup>-1</sup> (w), 1817 cm<sup>-1</sup> (m), 1803 cm<sup>-1</sup> (s).

**Synthesis of *cis*-Cyclic Cyclohexylcarbonate, **9**.**<sup>12</sup> This compound was synthesized by the same procedure as described for **1** by adding excess pyridine (3.75 g, 47.4 mmol) to a 10-mL CH<sub>2</sub>Cl<sub>2</sub> solution of *cis*-1,2-cyclohexanediol (0.60 g, 5.2 mmol). Upon

cooling in a dry ice/acetone bath, a 15-mL solution of triphosgene (1.08 g, 3.64 mmol) was added dropwise to the reaction mixture resulting in an orange solution followed by slow warming to room temperature. Workup of the product was analogous to the preparation of **1** but was recrystallized in ether/pentane to yield 0.45 g (87%). <sup>1</sup>H NMR (CDCl<sub>3</sub>): δ 1.35–1.70 (m, 4H, CH<sub>2</sub>), 1.90 (q, 4H, CH<sub>2</sub>), 4.71 (m, 2H, CH-carbonate). <sup>13</sup>C NMR (CDCl<sub>3</sub>): δ 23.01, 28.02, 83.32, 154.80. IR ν(C=O), CH<sub>2</sub>Cl<sub>2</sub>: 1869 cm<sup>-1</sup> (w), 1823 cm<sup>-1</sup> (sh), 1802 cm<sup>-1</sup> (s), 1793 cm<sup>-1</sup> (sh).

**Polymer Characterization.** Polymer samples were first characterized by <sup>1</sup>H NMR and IR spectroscopy. The amount of ether linkages was determined via <sup>1</sup>H NMR by integrating the peaks corresponding to the methine protons of the polyether at ~3.45 ppm and the polycarbonate at ~4.6 ppm. The presence or absence of the corresponding cyclic carbonate was investigated by monitoring the presence or absence of the ν(C=O) of the cyclic carbonate at ~1825 cm<sup>-1</sup>. Finally, M<sub>w</sub> and M<sub>n</sub> measurements were carried out at Exxon-Mobil using GPC.

**High Pressure in Situ Kinetic Measurements.** High pressure reaction kinetic measurements were carried out using a stainless steel Parr autoclave modified with a silicon probe to connect to the ASI ReactIR 1000 system. The rate of polymer and cyclic carbonate formation was monitored by repeating a typical polymerization run, except reducing the CO<sub>2</sub> pressure to 400 psi. The formation rates of the polycarbonate and the cyclic carbonate were monitored by following the ν(C=O) of the polycarbonate at ~1750 cm<sup>-1</sup> and of the cyclic carbonate at ~1825 cm<sup>-1</sup>.

**X-ray Crystallography.** A Bausch and Lomb 10× microscope was used to identify suitable colorless crystals of **1a**, **1a**·2THF, **2b**, and **8** from a representative sample of crystals of the same habit. The representative crystal was coated in a cryogenic protectant (i.e., mineral oil, paratone, or apezeon grease) and was then fixed to a glass fiber, which in turn was fashioned to a copper mounting pin. The mounted crystals were then placed in a cold nitrogen stream (Oxford) maintained at 110 K on a Bruker SMART 1000 three circle goniometer.

Crystal data and details of data collection for the complexes are provided in Table 1. The X-ray data were collected on a Bruker CCD diffractometer and covered more than a hemisphere of reciprocal space by a combination of three sets of exposures; each exposure set had a different φ angle for the crystal orientation,

(12) Burk, R. M.; Roof, M. B. *Tetrahedron Lett.* **1993**, *34*, 395.

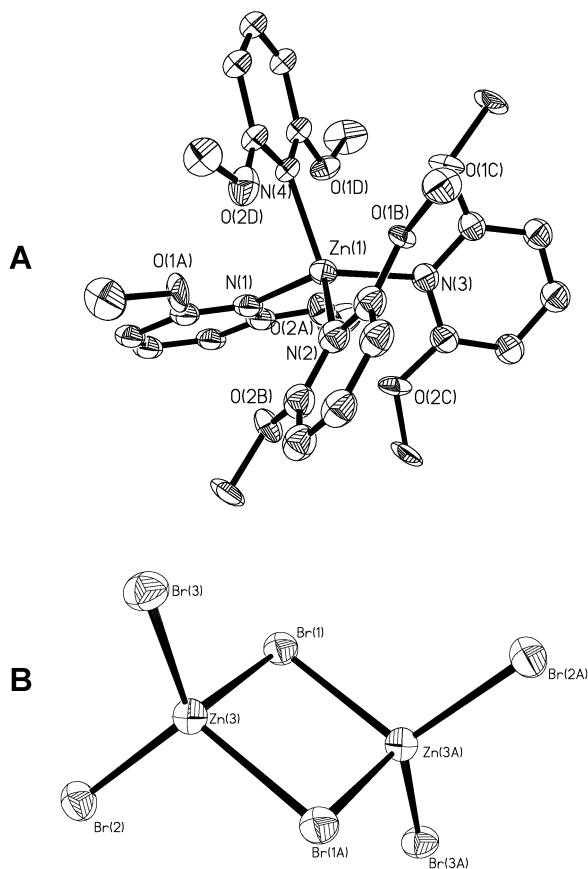


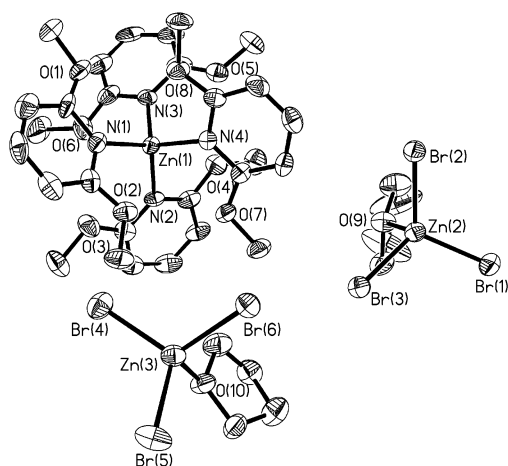
**Figure 1.** Thermal ellipsoid representation of complex **1a**. A.  $\text{Zn}(2,6\text{-dimethoxypyridine})_4^{2+}$ . B.  $\text{Zn}_2\text{Br}_6^{2-}$ . Average bond distances and bond angles in one of the *cations* are Zn–N (2.063[16] Å) and N–Zn–N (109.7–[7]°), whereas those in one of the *anions* are av terminal Zn–Br (2.350[3] Å), av bridging Zn–Br (2.501[3] Å), Br(1)–Zn(3)–Br(1A) (98.18(11)°, Br(2)–Zn(3)–Br(3) (120.97(13)°, Br(3)–Zn(3)–Br(1A) (107.76(11)°, Br(3)–Zn(3)–Br(1) (109.07(11)°, Br(2)–Zn(3)–Br(1) (107.67(12)°, and Br(2)–Zn(3)–Br(1A) (110.78(11)°).

and each exposure covered  $0.3^\circ$  in  $\omega$ . The crystal-to-detector distance was 4.9 cm. Crystal decay was monitored by repeating the data collection for 50 initial frames at the end of the data set and analyzing the duplicate reflections; crystal decay was negligible. The space group was determined on the basis of systematic absences and intensity statistics.

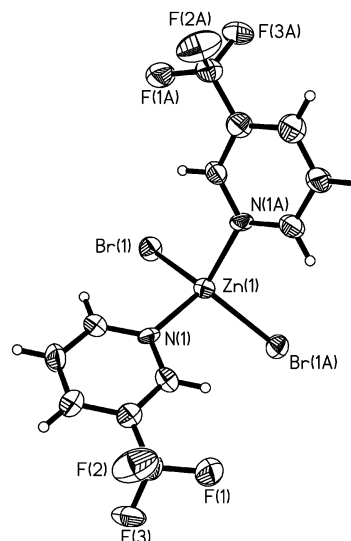
The structures were solved by direct methods. Full-matrix least-squares anisotropic refinement for all non-hydrogen atoms yielded  $R(F)$  and  $R_w(F^2)$  values as indicated in Table 1 at convergence. Hydrogen atoms were placed in idealized positions with isotropic thermal parameters fixed 1.2 or 1.5 times the value of the attached atom. Neutral atom scattering factors and anomalous scattering factors were taken from the International Tables for X-ray Crystallography Vol. C.

## Results and Discussion

The reactions of zinc halides ( $X = \text{Cl}, \text{Br}, \text{or I}$ ) and various 2,6-disubstituted pyridines have been carried out in the absence of highly coordinating solvents to afford salts of the form  $[\text{Zn}(\text{pyridine})_4][\text{Zn}_2\text{X}_6]$ . For example, X-ray quality crystals of  $[\text{Zn}(2,6\text{-dimethoxypyridine})_4][\text{Zn}_2\text{Br}_6]$  (**1a**) were obtained from diethyl ether, whereas, in THF, crystals of  $[\text{Zn}(2,6\text{-dimethoxypyridine})_4][\text{ZnBr}_3(\text{THF})]_2$  (**1a·2THF**) were isolated. Thermal ellipsoid representations of complexes **1a**



**Figure 2.** Thermal ellipsoid representation of complex **1a·2THF**. Average bond distances and bond angles in the *cation* are Zn–N (2.052[10] Å) and N–Zn–N (109.6[4]°), whereas those in the *anion* are Zn–Br (2.371[18] Å), Zn–O (2.110[8] Å), Br–Zn–Br (116.04[7]°), and O–Zn–Br (101.3–[2]°).

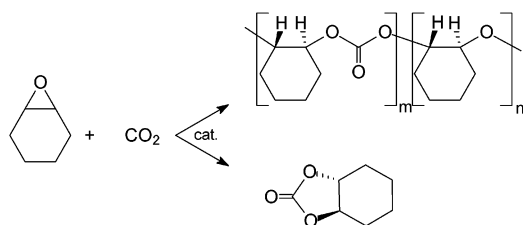


**Figure 3.** Thermal ellipsoid representation of complex **2b**. Zn–Br and Zn–N bond distances are 2.3746(17) Å and 2.084(12) Å, respectively, whereas the bond angles are N–Zn–N (117.3(6)°, Br–Zn–Br (127.44–(13)°, and av N–Zn–Br (103.3[3]°).

and **1a·2THF** with partial atom labeling schemes are depicted in Figures 1 and 2, where selected bond distances are also provided. On the other hand, the corresponding reactions of the zinc halides with 3-trifluoromethylpyridine yielded the simple  $\text{ZnX}_2(3\text{-trifluoromethylpyridine})_2$  complexes. It was possible to isolate X-ray suitable crystals of the derivative where  $X = \text{Br}$  (**2b**) by slow evaporation of methylene chloride from a concentrated  $\text{CH}_2\text{Cl}_2$  solution of the complex into toluene at  $-20^\circ\text{C}$ . The thermal ellipsoid drawing of **2b** may be found in Figure 3, along with selected bond distances and angles. As is evident from Figure 3, the zinc center in **2b** is of distorted tetrahedral geometry as expected for this type of complex.

Because of the effectiveness of pyridine derivatives of zinc halides for catalytically coupling carbon dioxide and propylene oxide to provide propylene carbonate, it was of interest to examine these complexes for the copolymerization

Scheme 1

**Table 2.** Catalytic Activity for the Copolymerization of Carbon Dioxide and Cyclohexene Oxide<sup>a</sup>

catalyst	% carbonate	TOF (g poly/g Zn/h) <sup>b</sup>
Zn <sub>3</sub> Cl <sub>6</sub> (2,6-dimethoxypyridine) <sub>4</sub>	80	27.1 (13.5)
Zn <sub>3</sub> Br <sub>6</sub> (2,6-dimethoxypyridine) <sub>4</sub>	85	27.5 (13.5)
Zn <sub>3</sub> I <sub>6</sub> (2,6-dimethoxypyridine) <sub>4</sub>	80	15.7 (7.9)
Zn <sub>3</sub> Br <sub>6</sub> (2-phenylpyridine) <sub>4</sub>	80	14.0 (7.1)
ZnBr <sub>2</sub> (3-trifluoromethylpyridine) <sub>2</sub>	91	1.87 (0.9)
ZnCl <sub>2</sub>	60	22 (11.6)

<sup>a</sup> Catalyst loading (0.100 g), 20.0 mL of cyclohexene oxide. Reaction conditions: 80 °C at a total pressure of 50 bar for a 24 h period. <sup>b</sup> TOF values in parentheses are in units of epoxide/mol of Zn/h.

of CO<sub>2</sub> and cyclohexene oxide. Indeed, regardless of the solid-state form of these zinc derivatives, that is, [Zn-(pyridine)<sub>4</sub>][Zn<sub>2</sub>X<sub>6</sub>] or Zn(pyridine)<sub>2</sub>X<sub>2</sub>, all complexes examined exhibited significant reactivity for affording poly(cyclohexylene carbonate) from CO<sub>2</sub>/cyclohexene oxide (Scheme 1). As noted in Scheme 1, these catalysts afford noticeable quantities of polyether linkages in the copolymers, as well as production of the minor product, *trans*-cyclic cyclohexylcarbonate. The copolymerization reactions were monitored in the ν(C=O) region of the infrared spectrum of the polycarbonate utilizing an in situ ASI 1000 ReactIR probe fitted to a modified 300 mL stainless steel Parr reactor. Figure 4 depicts a typical reaction profile as monitored by infrared spectroscopy for a reaction carried out at 80 °C in cyclohexene oxide at a CO<sub>2</sub> pressure of 30 bar. The major infrared absorption in the ν(C=O) region at ~1750 cm<sup>-1</sup> is for the polycarbonate, whereas the minor peak at ~1825 cm<sup>-1</sup> is due to the cyclic carbonate.

Table 2 summarizes the activity of several of these zinc halide catalysts, where complex **1a** displays the highest activity with a TOF of 27.5 g of polymer/g of zinc/h. Consistent with previously reported results for propylene carbonate production, the general trend observed is that the catalytic activity varies with halide, Cl ≈ Br > I, and the activity increases with increasing electron donating ability of the substituents on the pyridine ligands.<sup>10</sup> The highly active representative catalyst, complex **1a**, was employed to investigate the copolymerization process in more detail. As noted in Table 2, in neat cyclohexene oxide/CO<sub>2</sub>, the copolymer produced contained ~85% carbonate and ~15% ether linkages (see Figure 5). However, if the copolymerization process is carried out in a 2.5 M solution of cyclohexene oxide in toluene, the resulting copolymer contains essentially 100% carbonate linkages as indicated by the absence of the ether resonance in the <sup>1</sup>H NMR spectrum at 3.45 ppm (Figure 5). As expected under these conditions, the TOF is reduced to ~20 g of polymer/g of zinc/h. Similarly, if the copolymerization reaction is carried

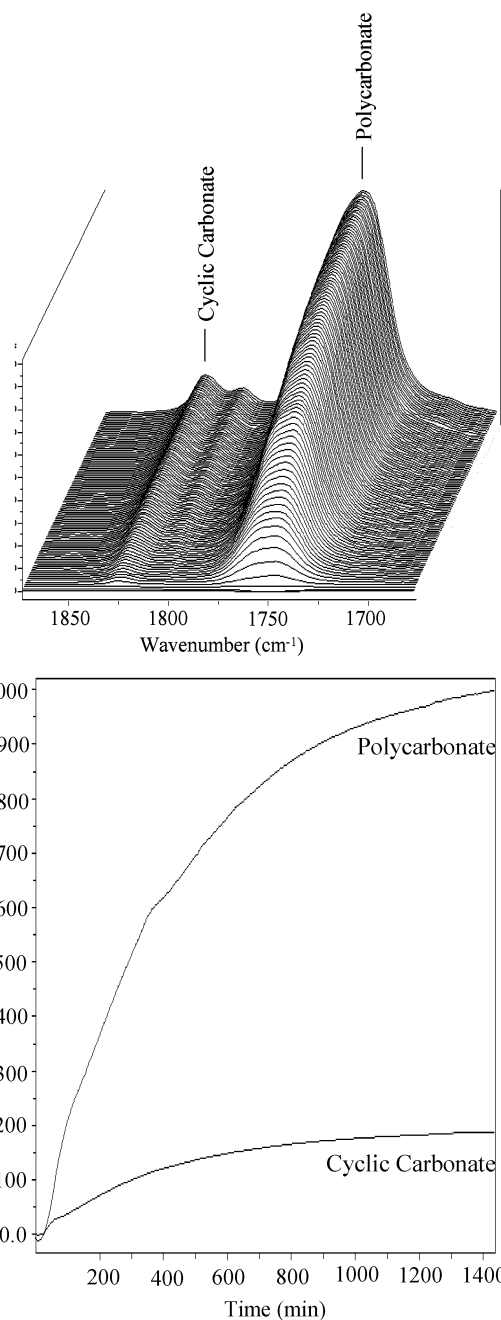


**Figure 4.** In situ infrared monitoring of the poly(cyclohexylene carbonate) and cyclic cyclohexylcarbonate formation as a function of time. Reaction run using complex **1a** as catalyst in CO<sub>2</sub> swollen cyclohexene oxide solution at 30 bar pressure and 80 °C.

out in a 10-fold excess of added pyridine ligand, the TOF is drastically reduced to ~5 g of polymer/g of zinc/h, but the carbonate content of the copolymer is ~100%. In these instances where copolymers were produced with 100% carbonate linkages, there was a concomitant increase in the molecular weights of the polymers. That is, the average  $M_n$  and  $M_w$  values were found to be 44 000 and 313 000, respectively, as compared to the corresponding molecular weights of 13 000 and 99 000 for the copolymers with 85% carbonate linkages.

As illustrated in Scheme 1, cyclic cyclohexylcarbonate (**8**) is observed as a minor product from the carbon dioxide/

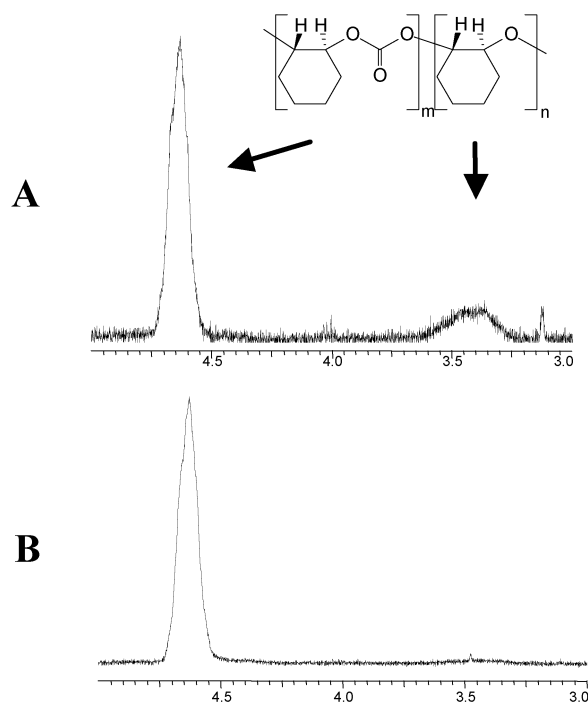


**Figure 5.**  $^1\text{H}$  NMR of poly(cyclohexylene carbonate). A. Reaction carried out in cyclohexene oxide. B. Reaction carried out in cyclohexene oxide with 10-fold excess of 2,6-dimethoxyppyridine added or in a 2.5 M solution of cyclohexene oxide in toluene.

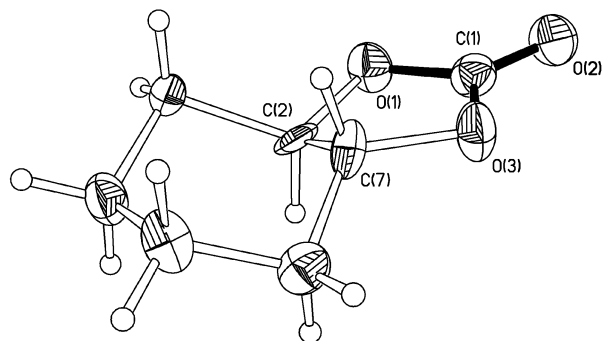


**Figure 6.** Thermal ellipsoid representation of *trans*-cyclic cyclohexylcarbonate. Selected bond distances and angles are the following: C(1)–O(2), 1.193(2) Å; C(1)–O(1), 1.346(2) Å; C(1)–O(3), 1.347(2) Å; C(2)–C(7), 1.501(6) Å, all other C–C bonds av 1.516[5] Å, and O(1)–C(1)–O(2), 124.14(18)°; O(2)–C(1)–O(3), 124.4(19)°; O(1)–C(1)–O(3), 111.44(16)°; O(3)–C(7)–C(2), 103.1(4)°; O(1)–C(2)–C(7), 101.2(4)°.

cyclohexene oxide coupling reaction. We were able to obtain crystals of **8** suitable for X-ray diffraction analysis by the slow evaporation of the methanol/ $\text{CH}_2\text{Cl}_2$  solution which remained upon removal of the high molecular weight copolymer. The thermal ellipsoid drawing of compound **8** is illustrated in Figure 6, along with the atomic numbering scheme and selected bond distances and angles. As expected, the cyclohexane ring carbon atoms are disordered (see Supporting Information). As noted in Figure 6, **8** is the *trans* isomer where there is significant strain in the five-membered ring of the carbonate. That is, the average deviation from the least squares plane defined by atoms O(1), O(3), C(1), C(2), C(7) is 0.116 Å, with the C(2) and C(7) atoms of the cyclohexane ring exhibiting the greater variations at  $-0.1642$  and  $0.1753$  Å, respectively. This ring strain is most likely the major factor which leads to the favorable production of

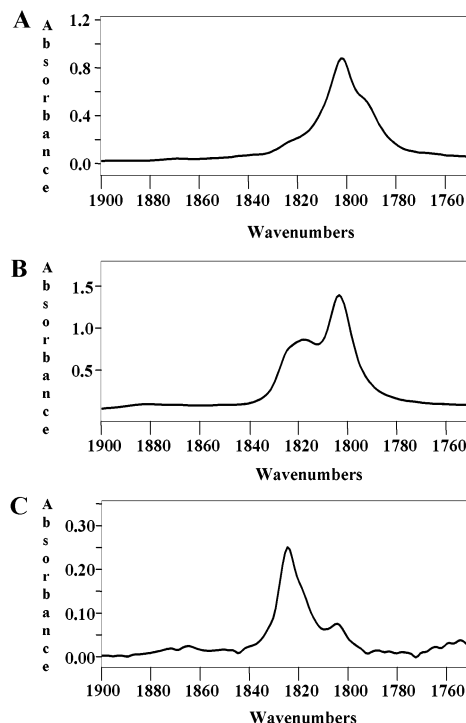


**Figure 7.** Infrared spectra in  $\nu(\text{C}=\text{O})$  region of cyclic cyclohexylcarbonate. A. *Cis* isomer in  $\text{CH}_2\text{Cl}_2$ . B. *Trans* isomer in  $\text{CH}_2\text{Cl}_2$ . C. *Trans* isomer in toluene.

copolymer versus cyclic carbonate observed when utilizing cyclohexene oxide as monomer. On the other hand, the corresponding five-membered ring of the cyclic carbonate derived from propylene oxide/ $\text{CO}_2$ , propylene carbonate, is perfectly planar.<sup>2f</sup> Consistent with this observation, the  $\text{CO}_2$ /propylene oxide coupling process carried out under similar reaction conditions utilizing **1a** as catalyst afforded mostly cyclic carbonate, with a minor product of copolymer. Indeed, this is consistent with what has been previously observed for other soluble catalyst systems.<sup>2</sup>

To definitively identify the stereochemistry of the cyclohexylcarbonate in solution by infrared and  $^{13}\text{C}$  NMR spectroscopy, we have independently synthesized both *cis* and *trans* isomers of cyclic cyclohexylcarbonate from the corresponding 1,2-cyclohexanediol and triphosgene by the established methods.<sup>12</sup> These data have allowed us to clearly establish that the *trans* isomer, compound **8**, is the sole carbonate produced from the reaction defined in Scheme 1. Figure 7 compares the infrared spectra in the  $\nu(\text{C}=\text{O})$  region for the *cis* and *trans* cyclohexylcarbonates in methylene chloride solvents. It should be noted, however, that the infrared spectra of cyclic cyclohexylcarbonates are highly solvent dependent.<sup>13</sup> For example, see the spectrum of *trans*-cyclohexylcarbonate obtained in toluene in Figure 7C, where the principal  $\nu(\text{C}=\text{O})$  frequency is  $\sim 1825\text{ cm}^{-1}$ , much like that observed in the  $\text{CO}_2$  swollen cyclohexene oxide solution (Figure 4).

(13) The infrared spectrum in the  $\nu(\text{C}=\text{O})$  region in methylene chloride of the cyclohexylcarbonate produced during the copolymer synthesis is identical to that for the pure *trans* isomer depicted in Figure 7B. In cyclohexene oxide and in toluene solutions, the spectra of *trans*-cyclohexylcarbonate are quite different from that observed in  $\text{MeCl}_2$  as is seen in Figures 7C and 8.

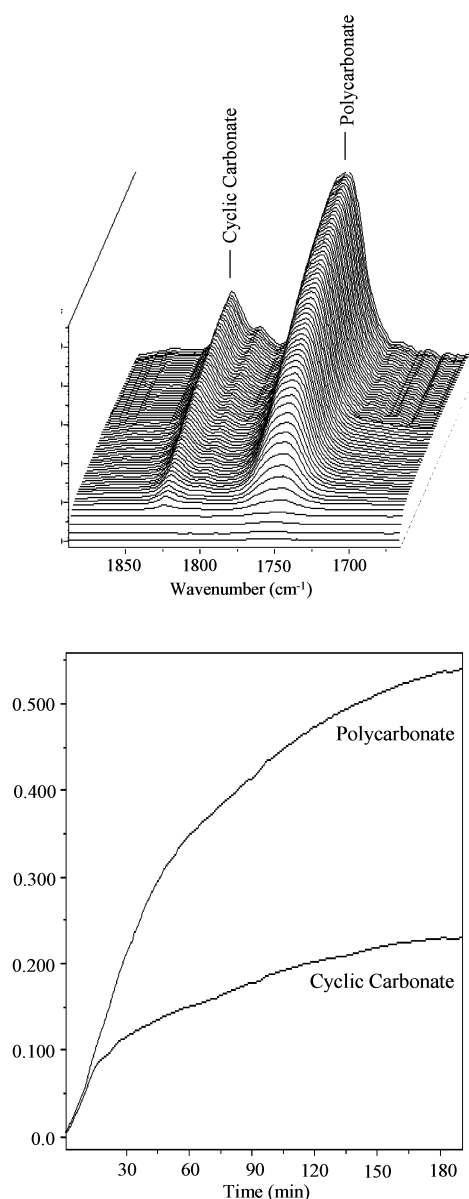


**Figure 8.** In situ infrared monitoring of the poly(cyclohexylene carbonate) and cyclic cyclohexylcarbonate formation as a function of time. Reaction performed using complex **1a** as catalyst in 2.5 M cyclohexene oxide in toluene at 55 bar pressure and 80 °C.

In an effort to better assess the mechanistic aspects of the copolymerization reaction involving cyclohexene oxide and carbon dioxide in the presence of one of these soluble zinc halide derivatives, specifically complex **1a**, we have performed kinetic measurements. These investigations were carried out at a total pressure of 30 bar and a temperature of 80 °C with the catalyst (or catalyst precursor) dissolved in a solution of cyclohexene oxide in toluene of known molarity. Reducing the CO<sub>2</sub> loading pressure to 10 bar did not significantly affect the rate of the reactions. An organic solvent was employed in these studies to ensure a single phase reaction system, where the concentrations of reagents could be more accurately controlled.<sup>14</sup> Additionally, under these conditions, copolymers containing 100% carbonate linkages are obtained. A representative series of infrared spectra for the cyclohexene oxide/carbon dioxide coupling

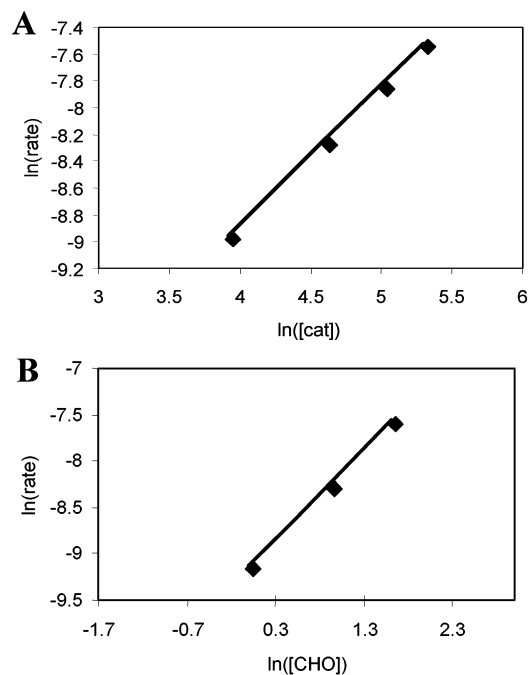


**Figure 9.** Plots of the ln[initial rate] of copolymer (poly(cyclohexylcarbonate) formation versus (A) ln **1a** and (B) ln[cyclohexene oxide]. Slope in part A = 1.03, and that in part B = 0.96.

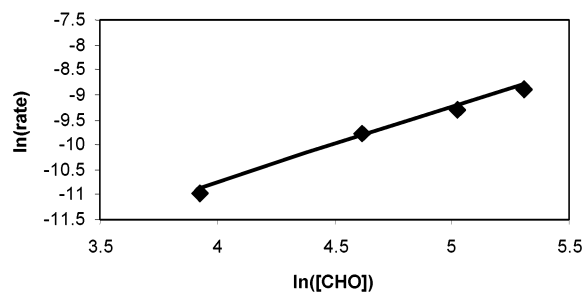


**Figure 10.** Plot of the ln[initial rate] of cyclic cyclohexylcarbonate formation versus ln **1a**. Slope = 1.50.

reactions is provided in Figure 8, where the  $\nu(\text{C}=\text{O})$  stretching vibrations are seen at  $\sim 1750$  and  $1825\text{ cm}^{-1}$  for the polycarbonate and cyclic carbonate, respectively. Figure 8 also illustrates the peak profiles as a function of time for production of both the major (poly(cyclohexenylene carbonate)) and minor (cyclic cyclohexylcarbonate) products. As is readily obvious from a comparison with the reactions monitored in the absence of organic solvent (Figure 4), in this instance there is a somewhat enhanced production of cyclic carbonate versus polycarbonate. The initial rates for the formation of poly(cyclohexylene carbonate) were determined as a function of [catalyst] and [cyclohexene oxide]. Plots of ln[initial rate] versus ln[catalyst] or ln[cyclohexene oxide] yielded slopes of unity, indicative of copolymer formation being first-order in both [catalyst] and [epoxide] (Figure 9). On the other hand, the initial rate of cyclic cyclohexylcarbonate formation is mixed-order in catalyst

(14) From studies of the phase behavior of the cyclohexene oxide–CO<sub>2</sub> binary,<sup>2c</sup> at 55 bar CO<sub>2</sub> pressure, there exist cyclohexene oxide-rich ( $X_{\text{CHO}}$  at 90 °C  $\approx 0.70$ ) and cyclohexene oxide-poor phases, the former being where the catalyst resides and the phase monitored by our in situ infrared probe.

Scheme 2

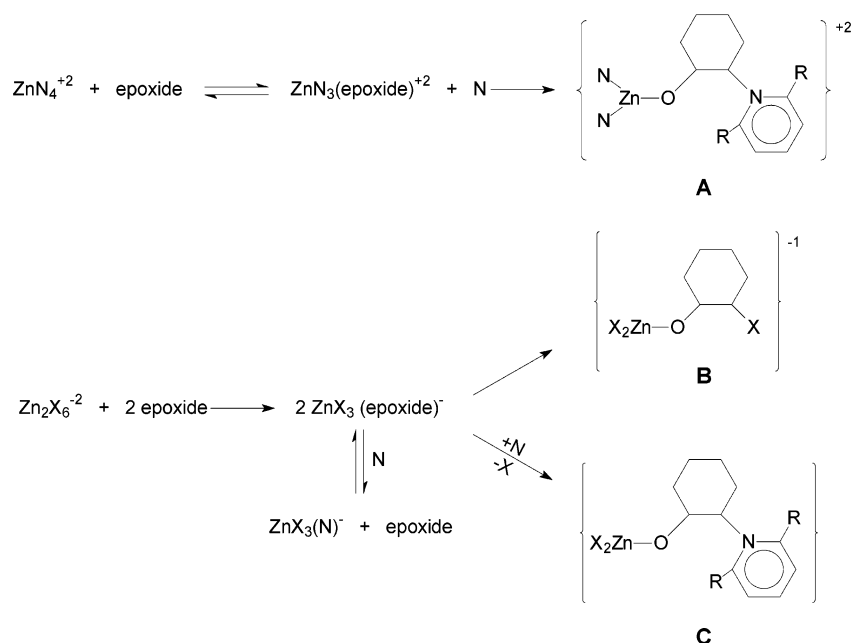


(Figure 10), that is, 1.50, suggesting involvement of both dimeric and monomeric zinc species as catalysts. This result is consistent with the enhanced rate of cyclic carbonate production in hydrocarbon solvent as compared to that in neat epoxide; that is, dimer formation would be favored in toluene (see Figures 4 and 8).

Finally, because zinc halides are molecular solids which are soluble in cyclic ethers, it was of interest to examine their ability in the absence of pyridine ligands to catalyze the homopolymerization of cyclohexene oxide to polyether or the copolymerization of cyclohexene oxide/ $\text{CO}_2$  to polycarbonates. Relevant to these processes, it is well-established that  $\text{ZnX}_2/(n\text{-Bu}_4\text{N})\text{X}$  salts catalyze the coupling of mono-substituted oxiranes to cyclic carbonates.<sup>9g</sup> In our study, the zinc halides were observed to readily homopolymerize cyclohexene oxide to polyether at ambient temperature. Upon reacting cyclohexene oxide and carbon dioxide in the presence of the zinc halides at 90 °C and 55 bar pressure, high molecular weight polycarbonates with substantial polyether linkages were produced with TOFs as high as 20 g of polymer/g of Zn/h. An analogous reaction involving  $\text{ZnCl}_2$  in the presence of the sterically demanding 2,6-di-*tert*-butylpyridine base gave identical results as the  $\text{ZnCl}_2$  only catalyzed process. Because of the high propensity of these salts for forming homopolymers, a sample of  $\text{ZnCl}_2$  was purified and sealed in a glass ampule which was broken after the addition of  $\text{CO}_2$  to the reaction system in order to minimize the production of polyethers. Even under these conditions, the resulting polymer contained ~30% ether linkages and ~70% carbonate linkages. These observations are consistent with the effectiveness of the pyridine ligands to increase the  $\text{CO}_2$  incorporation and TOFs of this catalyst system.

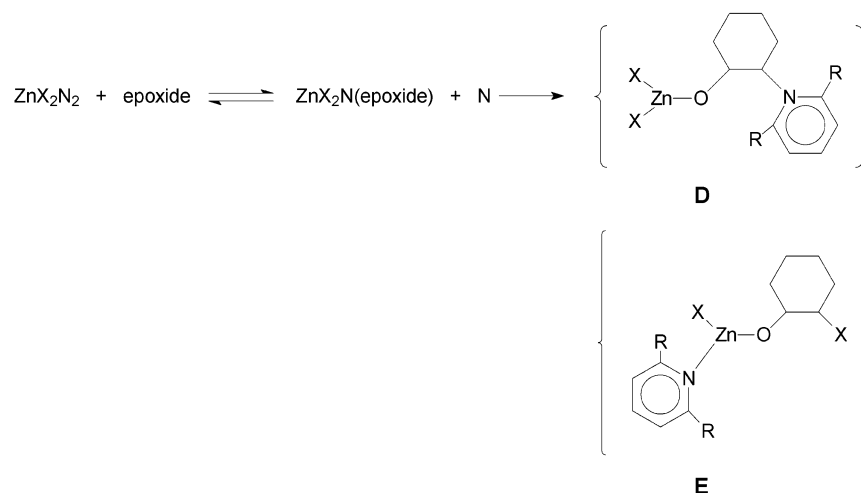
An array of possible intermediates in this carbon dioxide/epoxide coupling process can be proposed. In this regard, it should be noted that derivatives of  $[\text{Zn}(\text{pyridine})_4][\text{Zn}_2\text{X}_6]$ ,

where  $\text{Zn}_2\text{X}_6^{2-}$  reacts with cyclic ether (THF) to afford  $\text{ZnX}_3(\text{THF})^{1-}$ , or  $\text{Zn}(\text{pyridine})_4^{2+}$  undergoes ligand substitution with an oxygen donor ligand ( $\text{H}_2\text{O}$ ) yielding  $\text{Zn}(\text{pyridine})_3(\text{H}_2\text{O})^{2+}$ , have been fully characterized. In addition to the structures previously discussed, a related complex,  $[\text{Zn}(\text{2,6-dimethoxypyridine})_3\text{H}_2\text{O}][\text{Zn}_2\text{Br}_6]$ , **9**, was obtained from the reaction of  $\text{ZnBr}_2$  and 2,6-dimethoxy-pyridine where adventitious water was present. The crystal structure of this species was found to be similar to complex **1a** with the exception that one of the pyridine ligands on the zinc cation was replaced by a water molecule. A ball-and-stick drawing of the cation of this salt is provided in the Supporting Information. Nevertheless, some of these potential intermediates are more credible than others on the basis of known reactivity patterns. Schemes 2 and 3 contain possible candidates resulting from the intermediacy of  $\text{Zn}(\text{pyridine})_3(\text{epoxide})^{2+}$ ,  $\text{ZnX}_3(\text{epoxide})^{1-}$ , or  $\text{ZnX}_2(\text{pyridine})(\text{epoxide})$ .

For precursor complexes of the type  $[\text{Zn}(\text{2,6-R}_2\text{C}_5\text{H}_3\text{N})_4][\text{Zn}_2\text{X}_6]$ , potential intermediates in the copolymerization reactions are complexes **A**, **B**, and **C** as indicated in Scheme 2. These zinc species are derived from  $\text{Zn}(\text{2,6-R}_2\text{C}_5\text{H}_3\text{N})_3(\text{epoxide})^{2+}$  and  $\text{ZnX}_3(\text{epoxide})^{-1}$  which result from ligand substitution reactions at the zinc centers of the parent salts. Recall that analogues of these zinc derivatives have been identified for the oxygen donors  $\text{H}_2\text{O}$  and THF, respectively. Whereas the process affording **A** would not be expected to vary significantly with the nature of the halide counterion as is observed in Table 2, the process leading to **B** and **C** would be consistent with pyridine enhancing reaction rates and the nature of the copolymer thus produced as well as the fact that  $\text{ZnCl}_2$  alone is a good homopolymerization catalyst. Both processes would be first-order in complex **1a**. Furthermore, the cationic nature of **A** is not conducive to promoting the  $\text{CO}_2$  enchainment step. Furthermore,  $[\text{Zn}(\text{pyridine})_4][\text{BF}_4]_2$  was shown to be *inactive* as a catalyst for the copolymerization process. Alternatively, starting with



Scheme 3



$\text{ZnX}_2\text{N}_2$  precursors leads to species **D** which should readily lead to enchainment of both  $\text{CO}_2$  and epoxides. Indeed, the dimeric form of **D**, where the epoxide is propylene oxide, has been isolated and X-ray crystallographically characterized for the  $\text{CO}_2$ /propylene oxide coupling processes leading to cyclic carbonate.<sup>10</sup> The effect of added pyridine on the  $\text{CO}_2$  content of the polycarbonate is attributed to maintaining the active zinc center coordinatively saturated, thereby avoiding a consecutive epoxide ring-opening process. The rate decrease experienced in excess pyridine is readily accommodated in Schemes 2 and 3.

Finally, it is noteworthy that the zinc salts,  $[\text{Zn}(\text{pyridine})_4][\text{Zn}_2\text{X}_6]$ , do not undergo major ligand redistribution reactions at ambient temperature in cyclic ethers. For example,  $[\text{Zn}(\text{2,6-di-MeOC}_5\text{H}_3\text{N})_4][\text{ZnBr}_3(\text{THF})]_2$  was isolated from a THF solution of complex **1a**. Nevertheless, under the more rigorous reaction conditions of catalysis, it is possible that the zinc species in solution are quite different from the precursor complex.

### Summary

We have demonstrated herein that zinc halides in the presence of substituted pyridines lead to a variety of complexes involving zinc centers which contain quite different ligand sets, for example,  $\text{ZnX}_2(\text{pyridine})_2$  or  $[\text{Zn}(\text{pyridine})_4][\text{Zn}_2\text{X}_6]$  depending on the nature of the pyridine

ligand. Because of a lack of good spectral probes ( $^1\text{H}$  and  $^{13}\text{C}$  NMR) of these various zinc species in solution, all derivatives were characterized in the solid state by X-ray crystallography. These zinc complexes were shown to be catalytically active for the coupling of carbon dioxide and epoxides to provide high molecular weight polycarbonates and cyclic carbonates, with activity being greater for derivatives containing electron donating pyridine ligands. Although this investigation has not given rise to significantly more active or selective catalysts for the copolymerization of epoxides and carbon dioxide than those previously published, *the unique feature of these zinc catalyst precursors is their synthetic simplicity.*

**Acknowledgment.** Financial support from the National Science Foundation (Grants CHE-99-10342 and CHE 98-07975 for the purchase of X-ray equipment), and the Robert A. Welch Foundation, is acknowledged..

**Supporting Information Available:** Complete details (CIF format) of the X-ray diffraction studies on compounds **1a**, **1a·2THF**, **2b**, **8**, and **9**. Ball-and-stick representation of the cation of compound **9**. This material is available free of charge via the Internet at <http://pubs.acs.org>.

IC0259641